IOP Publishing Journal of Physics A: Mathematical and Theoretical

J. Phys. A: Math. Theor. **40** (2007) 13209–13215 doi:10.1088/1751-8113/40/44/002

A relationship of mean-field theory for a driven lattice gas to an exact equilibrium density functional

W S Brams Dwandaru[1,2] **and Matthias Schmidt**[1,3]

[1] H H Wills Physics Laboratory, University of Bristol, Tyndall Avenue, Bristol BS8 1TL, UK
[2] Physics Education Department, Yogyakarta State University, Yogyakarta, Indonesia
[3] Institut für Theoretische Physik II, Heinrich-Heine-Universität Düsseldorf, Universitätsstraße 1, D-40225 Düsseldorf, Germany

Received 17 July 2007, in final form 18 July 2007
Published 16 October 2007

Abstract

We consider the totally asymmetric exclusion process (TASEP) of particles on a one-dimensional lattice that interact with site exclusion and are driven into one direction only. The mean-field approximation of the dynamical equation for the one-particle density of this model is shown to be equivalent to the exact Euler–Lagrange equations for the equilibrium density profiles of a binary mixture. In this mixture particles occupy one (two) lattice sites and correspond to resting (moving) particles in the TASEP. Despite the strict absence of bulk phase transitions in the equilibrium mixture, the influence of density-dependent external potentials is shown to induce abrupt changes in the one-body density that are equivalent to the exact out-of-equilibrium phase transitions between steady states in the TASEP with open boundaries.

PACS numbers: 05.60.Cd, 61.20.Gy, 61.20.Lc

An important conceptual distinction between equilibrium and non-equilibrium statistical physics is often emphasized [1–4]: the former possesses a well-defined general theory, based on Gibbs ensembles, whereas the latter does not. In equilibrium cases density functional theory (DFT) provides a powerful framework for obtaining in principle all static properties of a system, in particular in inhomogeneous situations where the one-body density distribution varies in space [5, 6]. There is a variety of approaches that aim at generalizing DFT to non-equilibrium, such as the dynamic density functional theory (DDFT) by Kawasaki [7] and by Marconi and Tarazona [8, 9] and the time-dependent density functional theory (TDFT) [4] pioneered by Dieterich and co-workers. DDFT has been tested successfully in a variety of situations [10, 11], including non-equilibrium sedimentation of hard spheres under gravity, where excellent agreement with results from Brownian Dynamics computer simulations and from experiments using confocal microscopy of colloidal dispersions was found [12]. Nevertheless the DDFT is approximative [13, 14] and it is hence of practical interest to develop the framework further.

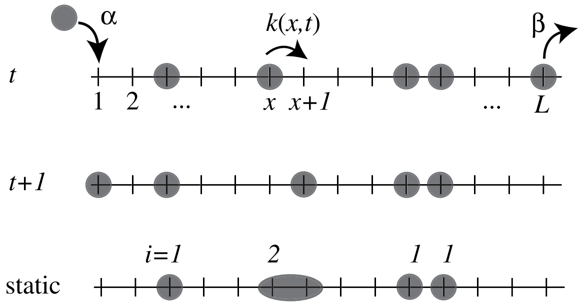

Figure 1. Illustration of the relationship between the TASEP and the hard core lattice gas. In the TASEP particles (grey dots) occupy a one-dimensional lattice, labelled by $x = 1, \ldots, L$. A particle can hop from site x to site $x + 1$ at rate $k(x, t)$. The system is coupled to an input and an output reservoir with rates α and β, respectively. In the equilibrium binary mixture particles on a lattice occupy one (species $i = 1$) or two (species $i = 2$) lattice sites. The position coordinate of the two particles is taken as the left excluded site.

Finding relationships between equilibrium and non-equilibrium situations is both of fundamental as well as of practical importance; the generalization of the Yang–Lee theory of equilibrium phase transitions to non-equilibrium transition by Blythe and Evans [15] is a primary example of such an achievement; see also [16, 17]. Here we investigate a relationship between inhomogeneous equilibrium and driven non-equilibrium systems using the specific example of a monomer-dimer hard core lattice fluid on the one hand and the totally asymmetric exclusion process (TASEP) on the other hand; both are simple one-dimensional models. The relationship is established via associating the one-body distribution functions of one model with those of the other and is (at present) of approximative nature. One particularly fascinating aspect is that DFT can be applied to examine the properties of the TASEP. Our arguments are general and we discuss their applicability to other models.

The TASEP has been studied extensively in the past as a fundamental model for one-dimensional transport [1–3, 18–23], with applications in intracellular transport, traffic and transport in porous media; exact solutions are known [22, 23]. Consider a one-dimensional lattice with L consecutive sites, labelled by $x = 1, \ldots, L$. At time t a particle can hop from site x to the neighbouring site $x + 1$ with rate $k(x, t)$ provided that site $x + 1$ is empty; here we have chosen formally the most general case and allow the hopping rate $k(x, t)$ to vary in space (see e.g. [24]) and time. We consider the case of open boundaries, where site 1 is filled with particles at rate α and site L is emptied with rate β; the upper two panels of figure 1 show an illustration. Introducing the occupation number $\tau(x, t)$ which is unity (zero) if site x is occupied (empty) at time t, the local instantaneous current distribution is given by the exact expression

$$j(x, t) = k(x, t)\langle\tau(x, t)(1 - \tau(x + 1, t))\rangle, \tag{1}$$

where $\langle\cdot\rangle$ denotes an average over an ensemble of realizations of the TASEP. The term on the right-hand side of equation (1) is the product of the hopping rate and the probability of site x being occupied while site $x + 1$ is empty; for this combination of occupation numbers a move from x to $x + 1$ is possible without violating the site exclusion condition. The time-resolved local density distribution is obtained as $\rho(x, t) = \langle\tau(x, t)\rangle$, and its time evolution is determined by requiring the local conservation of the number of particles, expressed as a continuity equation

$$\frac{\partial\rho(x, t)}{\partial t} = -\nabla j(x, t), \tag{2}$$

with the discrete partial derivatives defined as $\partial\rho(x,t)/\partial t = \rho(x,t+1) - \rho(x,t)$ and $\nabla j(x,t) = j(x+1,t) - j(x,t)$. The celebrated mean-field theory for the TASEP is obtained by assuming the factorization of the nearest neighbour occupancy correlations in equation (1), $\langle\tau(x,t)\tau(x+1,t)\rangle \approx \langle\tau(x,t)\rangle\langle\tau(x+1,t)\rangle = \rho(x,t)\rho(x+1,t)$, and hence taking the current distribution to be

$$j(x,t) = k(x,t)\rho(x,t)[1-\rho(x+1,t)]. \tag{3}$$

For steady states, where $\partial\rho(x,t)/\partial t = 0$ and hence $j(x,t) = \text{const}$, this theory predicts the exact out-of-equilibrium phase diagram of the TASEP as a function of the boundary rates α and β [18, 25] (discussed below). Corresponding results for the (inhomogeneous) density profiles are approximative.

Density functional theory (DFT) is a powerful tool for investigating equilibrium properties, in particular of inhomogeneous systems that are exposed to the influence of external potentials $V_i^{\text{ext}}(x)$ acting on species i (in the case of mixtures) [5, 6]. Here we focus on one-dimensional lattice systems with space coordinate $x = 1,\ldots,L$ as above and denote the occupation numbers of species i at site x by $\tau_i(x)$. As we treat static properties, there is no dependence on time t. Particles interact with pairwise interaction potentials $V_{ij}(x,x')$ that act between a particle of species i at site x and a particle of species j at site x' (and considering $x < x'$ suffices). The density profile of species i is the grand canonical average $\rho_i(x) = \langle\tau_i(x)\rangle$, and we restrict ourselves in the following to binary mixtures such that $i = 1, 2$. In DFT the grand potential is expressed as a functional of the one-body density distributions, $\rho_1(x)$ and $\rho_2(x)$, as

$$\tilde{\Omega}([\rho_1,\rho_2],\mu_1,\mu_2,T,L) = F([\rho_1,\rho_2],T,L) + \sum_{i=1,2}\sum_{x=1}^{L}\left(V_i^{\text{ext}}(x) - \mu_i\right)\rho_i(x), \tag{4}$$

where $F([\rho_1,\rho_1],T,L)$ is the Helmholtz free energy functional[4], μ_i is the chemical potential of species $i = 1, 2$ and T is temperature. The equilibrium density distributions are those that minimize the grand potential, i.e. that fulfil the Euler–Lagrange equations

$$\frac{\delta\tilde{\Omega}([\rho_1,\rho_2],\mu_1,\mu_2,T,L)}{\delta\rho_i(x)} = 0, \qquad i = 1, 2. \tag{5}$$

The value of the grand potential at equilibrium, Ω, is obtained by inserting the solutions of equation (5) for $\rho_1(x)$ and $\rho_2(x)$ into the grand potential functional, equation (4), i.e. $\Omega(\mu_1,\mu_2,T,L) = \tilde{\Omega}([\rho_1,\rho_2],\mu_1,\mu_2,T,L)$. The Helmholtz free energy functional F is conveniently split into the free energy functional of an ideal gas (second term on the right hand side below) and an excess (over ideal) part, F_{exc}, that is due to interactions between the particles:

$$F([\rho_1,\rho_2],T,L) = F_{\text{exc}}([\rho_1,\rho_2],T,L) + k_{\text{B}}T\sum_{i=1,2}\sum_{x=1}^{L}\rho_i(x)(\ln(\rho_i(x)) - 1), \tag{6}$$

where k_{B} is the Boltzmann constant. The framework as outlined above is exact. In typical applications, $F_{\text{exc}}[\rho_1,\rho_2]$ is unknown for a given model fluid (specified by $V_{ij}(x,x')$), and one has to rely on an approximation for it in order to calculate density profiles and the grand potential (and hence all thermodynamic quantities) for given external potentials $V_i^{\text{ext}}(x)$ via solving (possibly numerically) equation (5).

[4] Strictly speaking, for lattice models $\tilde{\Omega}$ and F are not functionals but rather functions of the discrete set of variables $\{\rho_1(1),\rho_1(2),\ldots,\rho_1(L),\rho_2(1),\rho_2(2),\ldots,\rho_2(L)\}$; the continuum notation is used for convenience and to highlight the analogy of the continuum and the discrete cases.

In the following we apply DFT to an equilibrium mixture of small (species 1) and large (species 2) hard core particles that occupy one and two lattice sites, respectively. This model can be viewed as a discrete version of the Tonks gas [26]. In detail, the interactions between particles are such that a particle at site x excludes particles of both species from site x and that a particle of species 2 at site x additionally excludes particles of both species from site $x+1$. These exclusion rules are equivalent to pair potentials given by $V_{11}(x,x') = \infty$ if $x = x'$ and zero otherwise; $V_{12}(x,x') = \infty$ if $x = x'$ and zero otherwise; $V_{21}(x,x') = \infty$ if $x' - x \leqslant 1$ and zero otherwise; and $V_{22}(x-x') = \infty$ if $x' - x \leqslant 1$ and zero otherwise. The *exact* excess free energy functional for this model [27–29] is given by

$$F_{\text{exc}}[\rho_1, \rho_2] = k_B T \sum_{x=1}^{L} [\Phi_0(\rho_1(x) + \rho_2(x) + \rho_2(x+1)) - \Phi_0(\rho_2(x))], \tag{7}$$

where the function $\Phi(\cdot)$ is given by $\Phi_0(\eta) = (1-\eta)\ln(1-\eta) + \eta$ and can be interpreted as the excess free energy density of a 'zero-dimensional' system, i.e. that of an isolated site with mean occupancy number η. Using equations (4) and (6) and carrying out the derivatives in equation (5) yields the two Euler–Lagrange equations

$$\rho_1(x) = z_1(x)[1 - \rho_1(x) - \rho_2(x-1) - \rho_2(x)], \tag{8}$$

$$\rho_2(x) = z_2(x) \frac{[1 - \rho_2(x) - \rho_2(x+1) - \rho_1(x+1)][1 - \rho_2(x-1) - \rho_2(x) - \rho_1(x)]}{1 - \rho_2(x)}, \tag{9}$$

where $z_i(x) = \exp\left(\left(\mu_i - V_i^{\text{ext}}(x)\right)/k_B T\right)$ is the local fugacity of species i at site x. To lowest order in $\rho_2(x)$, corresponding to neglecting interactions between particles of species 2, one can simplify equations (8) and (9) to obtain

$$z_1(x) = \frac{\rho_1(x)}{1 - \rho_1(x)}, \tag{10}$$

$$\rho_2(x) = \frac{z_2(x)}{z_1(x)} \rho_1(x)[1 - \rho_1(x+1)]. \tag{11}$$

We are now in a position to detail the relationship between the two models. Our key finding is that the linearized Euler–Lagrange equation for species 2, equation (11), becomes equivalent to the mean-field expression for the current in the TASEP, equation (3), upon making the following identification of the fields of the two models:

$$\rho_1(x,t) = \rho(x,t), \tag{12}$$

$$\rho_2(x,t) = j(x,t), \tag{13}$$

$$\frac{z_1(x)}{z_2(x)} = k(x,t). \tag{14}$$

This mapping exploits an intuitive similarity of the binary mixture and the TASEP: small particles in the binary mixture resemble particles at rest in the TASEP, equation (12). Large particles in the binary mixture resemble particles in the TASEP that move (and hence contributes to the current), equation (13); this is because a successful move from x to $x+1$ implies that site x is occupied and site $x+1$ is empty—a configuration that is enforced in the binary mixture by the extended size of the particle of species 2, see figure 1. The ratio $z_1(x)/z_2(x)$ is the Boltzmann factor of the free energy cost of an identity (species) exchange of a particle at position x, and is hence intimately related to the hopping rate in the TASEP, equation (14), because moving a particle at site x corresponds to choosing a particle at rest

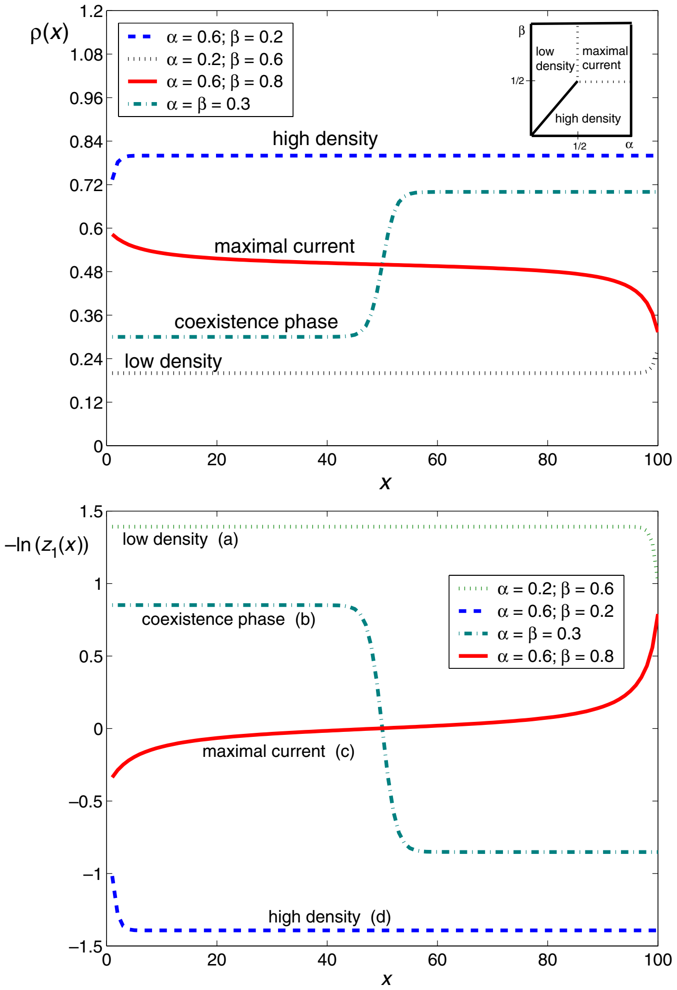

Figure 2. Upper panel. Representative density profiles $\rho(x)$ as a function of position x for the TASEP with open boundaries. Results are obtained from mean-field theory for a system of size $L = 100$ in the high density phase ($\alpha = 0.6, \beta = 0.2$, dashed line), low density phase ($\alpha = 0.2, \beta = 0.6$, dotted line), maximal current phase ($\alpha = 0.6, \beta = 0.8$, solid line) and coexistence between high and low density phases ($\alpha = \beta = 0.3$, dash-dotted line). The inset shows the out-of-equilibrium phase diagram of the TASEP as a function of α and β including high density, low density, maximal current and coexistence (thick line) phases. Lower panel. Local fugacities $z_1(x)$ of small particles that generate the same density profiles for species 1, $\rho_1(x)$, as shown in the upper panel.

(This figure is in colour only in the electronic version)

(species 1) and transforming it into a particle that moves (species 2), see the Lower panel of figure 1. We note further that using equation (12) the right-hand side of equation (10) becomes $\rho(x)/(1-\rho(x))$ which is known as the 'auxiliary field' in the mean-field theory for the TASEP, which we recover here as the local fugacity $z_1(x)$ in the binary mixture.

To illustrate the correspondence between the two models, we have calculated the one-body distributions for four typical steady states, as characterized by the input and output rates, α and β, see figure 2. Results from two different numerical methods agree, that is from numerical minimization of the density functional, using Picard iteration, and from using a recursion formulation of the mean-field equation for the TASEP. The inhomogeneous local fugacity $z_1(x)$ of small particles (shown in the lower panel of figure 2) generates the same density profile for species 1, $\rho_1(x)$, as shown in the upper panel for each of the four cases. The non-equilibrium phase diagram of the TASEP includes maximal current phase, high-density, low-density phase and coexistence between the latter, as a function of α and β (see the inset of figure 2). The phase diagram as obtained from the mean-field theory is exact. It is worth emphasizing that the DFT generates the same phase diagram; this seems at first sight to contradict the rigourous absence of equilibrium phase transitions in one-dimensional models with short-ranged interparticle forces (for a discussion see e.g. [30]). However, closer inspection resolves this puzzle, as the equilibrium problem is stated in a slightly non-standard way. Note that the steady-state condition $j(x,t) = \text{const}$ translates via (12) to $\rho_2(x) = \text{const}$. Hence the equilibrium problem consists of solving for $\rho_1(x)$ and $z_1(x)$ given a known field $z_1(x)/z_2(x)$ and the above condition $\rho_2(x) = \text{const}$. Hence the apparent phase transitions are generated by sudden changes in the external fields $z_1(x)$ and $z_2(x)$. Note that the profiles shown in figure 2 are approximate (in particular the exact profile of the coexistence phase has a linear dependence on x).

We are now in a position to generalize the considerations above and to outline a DFT-based approach for driven lattice models other than the simple TASEP, i.e. models that include particles of arbitrary size [31], mixtures of different species, as well as higher spatial dimensions [32]. Given such a model the following steps need to be carried out. (i) To treat particles at rest as species 1 (monomers in the example above) and to introduce new species i that correspond to moving particles; for hard core models the shape of those particles is obtained from 'fusing' the particle shape before the move and that after the move (species 2 of dimers in the example above). (ii) To treat the equilibrium mixture with DFT. There is a variety of approaches to obtain approximate DFTs in cases where the exact free energy functional is unknown; the recent lattice fundamental measure theory [28, 29] provides a particularly powerful means to construct systematically such approximations. (iii) To obtain the Euler–Lagrange equations for the mixture and to identify the hopping rate in the direction i with the ratio of fugacities z_i/z_1, where z_1 is the local fugacity of species 1, and z_i is the local fugacity of species i.

As an example we sketch the application to the TASEP in two spatial dimensions [32], where particles are driven on a square lattice (x, y) with rate $k(x, y, t)$ in the positive x direction and behave diffusively in the y direction, i.e. jump with rate $k'(x, y, t)$ in the positive or negative y direction. We keep the above monomers (species 1) and dimers (species 2), and introduce two further quasi-species, whose particles correspond to moves in the positive y direction (species 3) and negative y direction (species 4). The hard core pair interactions model dimers that are aligned along the y direction and are such that particles of species 3 occupy sites (x, y) and $(x, y+1)$ and particles of species 4 occupy sites (x, y) and $(x, y-1)$. The approach of [28, 29] is well suited to formulate a DFT for this four-component mixture. As above, the density profile of species 2, $\rho_2(x, y)$, is identified with the (partial) current across the 'bond' (x, y) to $(x+1, y)$. The density profiles of the new species correspond to the partial current from (x, y) to $(x, y+1)$ (species 3) and from (x, y) to $(x, y-1)$ (species 4). The hopping rates are associated with the local fugacities via $k(x, y, t) = z_1(x, y)/z_2(x, y)$ and $k'(x, y, t) = z_1(x, y)/z_3(x, y) = z_1(x, y)/z_4(x, y)$, where z_i is the local fugacity of species i at site (x, y). How such applications compare to mean-field theories obtained from factorization of correlations (e.g. generalizations of equation (3) to higher dimensions) remains to be seen and will be the object of further studies. One might hope that the consistency inherent in equilibrium DFT proves advantageous, in particular in the case of more complicated models than those considered here.

As a further outlook, it might be interesting to investigate whether one might be able to find, at least on a formal level, a density functional representation that is equivalent to the exact equations of motion of the one-dimensional TASEP, equation (1), rather than the mean-field version (3).

Acknowledgments

We acknowledge useful discussions with A Maciołek, D Mukamel, N B Wilding J F Annett, A J Archer, R Evans and R M L Evans. M S thanks the EPSRC and the German Science Foundation (DFG-SFB TR6/D3) for support. W S B D thanks the British Council for support through a Chevening Scholarship.

References

[1] Schmittmann B and Zia R 1995 *Phase Transitions and Critical Phenomena* ed C Domb and J L Lebowitz (London: Academic)
[2] Mukamel D 2000 *Soft and Fragile Matter: Nonequilibrium Dynamics, Metastability and Flow* ed M E Cates and M R Evans (Bristol: Institute of Physics Publishing) p 205, see also*Preprint* cond-mat/0003424
[3] Helbing D 2001 *Rev. Mod. Phys.* **73** 1067
[4] Gouyet J, Plapp M, Dieterich W and Maass P 2003 *Adv. Phys.* **52** 523
[5] Evans R 1979 *Adv. Phys.* **28** 143
[6] Evans R 1992 *Fundamentals of Inhomogeneous Fluids* ed D Henderson (New York: Dekker) chapter 3, p 85
[7] Kawasaki K 1994 *Physica* A **208** 35
[8] Marini Bettolo Marconi U and Tarazona P 1999 *J. Chem. Phys.* **110** 8032
[9] Marini Bettolo Marconi U and Tarazona P 2000 *J. Phys.: Condensed Matter* **12** A413
[10] Dzubiella J and Likos C N 2003 *J. Phys.: Condensed Matter* **15** L147
[11] Penna F, Dzubiella J and Tarazona P 2003 *Phys. Rev.* E **68** 061407
[12] Royall C P, Dzubiella J, Schmidt M and van Blaaderen A 2007 *Phys. Rev. Lett.* **98** 188304
[13] Archer A J and Evans R 2004 *J. Chem. Phys.* **121** 4246
[14] Chan G K L and Finken R 2005 *Phys. Rev. Lett.* **94** 183001
[15] Blythe R A and Evans M R 2003 *Braz. J. Phys.* **33** 464
[16] Brak R, de Gier J and Rittenberg V 2004 *J. Phys. A: Math. Gen.* **37** 4303
[17] Blythe R A, Janke W, Johnston D A and Kenna R 2004 *J. Stat. Mech.* JSTAT10(2004) P10007
[18] Krug J 1991 *Phys. Rev. Lett.* **67** 1882
[19] Tilstra L G and Ernst M H 1998 *J. Phys. A: Math. Gen.* **31** 5033
[20] Chowdhury D, Santen L and Schadschneider A 2000 *Phys. Rep.* **329** 199
[21] Hinsch H and Frey E 2006 *Phys. Rev. Lett.* **97** 095701
[22] Derrida B, Domany E and Mukamel D 1992 *J. Stat. Phys.* **69** 667
[23] Derrida B, Evans M R, Hakim V and Pasquier V 1993 *J. Phys. A: Math. Gen.* **26** 1493
[24] Lakatos G, Chou T and Kolomeisky A 2005 *Phys. Rev.* E **71** 011103
[25] Kolomeisky A B, Schütz G M, Kolomeisky E B and Straley J P 1998 *J. Phys. A: Math. Gen.* **31** 6911
[26] Tonks L 1936 *Phys. Rev.* **50** 955
[27] Percus J K 1976 *J. Stat. Phys.* **15** 505
[28] Lafuente L and Cuesta J A 2002 *Phys. Rev. Lett.* **89** 145701
[29] Lafuente L and Cuesta J A 2004 *Phys. Rev. Lett.* **93** 130603
[30] Cuesta J A and Sánchez A 2004 *J. Stat. Phys.* **115** 869
[31] Lakatos G and Chou T 2003 *J. Phys. A: Math. Gen.* **36** 2027
[32] Alexander F J, Cheng Z, Janowsky S A and Lebowitz J L 1992 *J. Stat. Phys.* **68** 781